A Local Cellular Model for Growth on Quasicrystals

Prince Chidyagwai

Box 7688, Lafayette College, Easton, PA, 18042 USA

Clifford A. Reiter

Department of Mathematics, Lafayette College, Easton, PA, 18042 USA

Abstract

The growth of real valued cellular automata using a deterministic algorithm on 2–dimensional quasicrystalline structures is investigated. Quasicrystals are intermediate between the rigid organization of crystals and disorganized random structures. Since the quasicrystalline structures may be highly symmetric or not, we are able to obtain highly organized and relatively random growth patterns. This deterministic growth produces dendrite, sector, stellar, regular polygons, round, and random DLA-like structures.

Introduction

Cellular automata are discrete dynamical systems whose behavior depends on local rules. Perhaps the most famous cellular automata is The Game of Life described by John Conway [1,2]. That automaton remains intriguing because its complex behavior is capable of universal computation. However, more serious applications are becoming common because cellular automata allow parallel processing [3]. Real valued cellular automata are also commonly used in applications such as image processing [4]. Such automata were used as a local model for snow crystal growth on a hexagonal lattice [5]. A wide range of growth structures were created, including stellar, dendrite, sector, and

plate forms which includes the basic 2-dimensional types seen in physical snowflakes. Of course, the growth exhibited, and was limited to, having 6-fold symmetry as determined by the underlying lattice. In this paper we investigate a similar growth model on more general underlying structures that allow us to obtain *n*-fold symmetry as well as randomness.

Quasicrystals are usually recognized by having diffraction patterns with a rotational symmetry that could not result from a crystalline structure. More directly, typical quasicrystalline structures are recognized by their local repetitiveness and their lack of the translational periodicity property of crystals. Thus quasicrystals are intermediate between crystals and random structures. Quasicrystals may or may not have global rotational symmetry and the symmetries are not restricted as they are for crystal growth. The only global rotational symmetry that is compatible with crystalline structures are 2-fold, 3-fold, 4-fold and 6-fold rotations [6]. However, quasicrystalline structures may be created with any other *n*-fold rotational symmetry. For example, the first tiling in Figure 1 shows a quasicrystalline tiling similar to a Penrose tiling. Its diffraction pattern has 5-fold symmetry forbidden for crystalline structures, nonetheless, it has no global symmetry. The second tiling in Figure 1 shows a quasicrystalline structure with 8-fold global symmetry but without translational symmetry. Thus we will be able to create deterministic growth patterns with symmetries forbidden for crystals. As in the hexagonal case, we see dendritic, stellar, sector, and plate growth but with new rotational symmetries. We will also see that quasicrystalline deterministic growth can appear quite similar to diffusion limited aggregation (DLA). DLA growth is based upon probabilistic

growth [7,8]. Our model also allows 2-dimensional circular clump-like growth similar to graupels which are naturally occurring snow crystals not modeled in [5].

Weeks [9] has also investigated automata on quasicrystalline structures, but not yielding growth as investigated here.

Model and Parameter Diagram

Snow crystals are intriguing because they have striking 6-fold symmetry and a diversity of forms, including highly complex forms. These have been recorded in photographs [10,11], and studied in a laboratory [12]. The diversity of snow crystal forms includes 2-dimensional and 3-dimensional forms. Nakaya replicated those forms in the laboratory by varying the temperature of air and a water bath that introduced water vapor. Hence we view the process as having two essential parameters roughly corresponding to temperature and saturation. Many other models of crystal growth are essentially based upon random processes [7,8]. A simple local deterministic model for the 2-dimensional ice crystal forms was described in [5] and this note generalizes that to quasicrystalline structures.

That model can be described as follows, each cell contains a real value with values greater than or equal to 1 corresponding to solid material and values less than 1 corresponding to material that is in a fluid state. Cells are called receptive if they are either solid or they have at least one solid neighbor. Other cells are nonreceptive. The updated values are the sum of two quantities. Very informally, we consider the two quantities as giving the material bound to the solid cells plus material moved by diffusion of the unbound material. The first quantity is the value of the receptive cell plus a

constant, γ, if the cell was receptive; otherwise the first quantity is zero. The second quantity is an average of the nonreceptive values where receptive sites have been replaced by zero. The average we compute is ½ of the value of the cell plus ½ the average value of its neighbors. This average is computed for all cells and using all cells except that the values of receptive sites have been replaced by zero. Figure 2, which is from [5], illustrates the process on a small hexagonal patch. In this note we will only consider the above type of averaging. However, these averages are not usually the optimal approximation to the Laplacian (which is ordinarily used to model diffusion) at any one quasicrystalline vertex, but nonetheless, these averages are close and model diffusion of the free material. We note that in [5] it was seen that the particular details of growth are extremely sensitive to the averaging coefficients although small changes in coefficients usually maintain the same overall qualitative behavior.

While originally applied only to hexagonal structures, we have described the above algorithm so that it can be applied to any graph (with finite degree). In particular, in this paper we investigate this growth model on 2-dimensional quasicrystalline structures created in the manner of [13]. That is, we use canonical projections with shifts as described there and which give rise to crystalline and quasicrystalline structures with different local patches of regularity and global symmetries. In this paper we will always use a shift in Z_n so that there is global *n*-fold rotational symmetry in the resulting structure on which the automata runs. The vertices of the quasicrystalline structure are the cells of our automata, and edges correspond to the neighbors in the automata. Since these structures have *n*–fold rotational symmetry, we refer to the vertex at the center of the symmetry as the center of the growth model. While typical tiling images such as Figure 1

have a few thousand vertices, for our growth model experiments, we utilize quasicrystalline structures with hundreds of thousands of vertices.

As a first example, consider the quasicrystalline structure generated by Z_5 with shift chosen so that the structure has a 5-fold rotational symmetry. We initialize this structure by setting all cells to a value β except the center cell which is set to 1. Thus we have a single solid particle immersed in a bath of level β. Figure 3 shows a diagram illustrating the growth for various β and γ values. The growth was run for 10,000 iterations or until solid material approached the boundary. The boundary was maintained at the constant level β. The solid material is shown with gray scales from half grey up to white, with white being closest to level 1. Nonsolid material is shown with grey scales from black to half grey with, black corresponding to level 0. Thus, there is a jump in grayscale at the boundary between solid and fluid material.

A decagonal plate appears whenever γ is 1 regardless of the value of β. Otherwise, increasing β and γ tends to give fuller growth; intermediate levels of β and low γ give rise to dendritic growth. Various sector, stellar and graupel forms are also visible. When $\beta = 0.75$ and $\gamma = 0.001$ the structure has a circular appearance similar to graupels. When β and γ are both small the growth is very slow. For a more extensive parameter table see [14].

The growth rate of various statistics of the model can be measured. There are two natural measures on the underlying quasicrystalline structures: the graph sense of distance that results from counting the number of edges traversed and the Euclidean distance of the embedding of the graph in the plane. In our experience the choice does not change the general tendencies of the statistics. Since it is easiest to describe the edge cells

for the graph measure, we will use that sense of distance. In particular, we will consider a cell to be an edge cell if it is ice but it has some neighbors that are not ice.

Most of the growth statistics we measured were unsurprising. For example, the number of cells that are ice tends toward growing quadratically with time. The number of edge vertices grows in a more diverse way depending upon the fractal nature of the growth. For example, when $\beta = 0.45$ and $\gamma = 0$, the growth is dendritic which has a fractal quality. Figure 4 shows a log-log plot of the number of edge vertices versus time for this growth. The growth seems to have an asymptotic slope which corresponds to the growth exponent. When a fit is done on the trailing half of points, we get an estimate for the exponent of 1.84. Hence the number of edge cells grows roughly like $Ct^{1.84}$. Thus, the fractal growth of the edge is near but below quadratic growth in that case. Figure 5 shows the fractional exponent for $\gamma = 0$ as β varies. Thus the edge appearing in the thick growth at the top of Figure 3 has a fractal dimension very near 2. Figure 6 shows the fractional exponent for $\beta = 0.45$ as γ varies although a non-uniform scale is used to emphasize the spike near $\gamma = 0$. Thus, the edges of the plates on the right of Figure 3 grow linearly, as expected.

Variation on Symmetry

Selected examples of the growth model on quasicrystalline structures generated by Z_5 to Z_8 are shown in Figure 7. Dendritic growth with 10 branches occurs when $n = 5$; notice that the branches themselves are not symmetric and that there are reflections between the branches. Thus the $n = 5$ figures have dihedral D_5 symmetry despite having 10 branches. The $n = 6$ structure generated via canonical projection is

actually a crystalline structure; however, it is not the complete hexagonal lattice. The $n = 6$ illustrations in Figure 7 also show dendritic growth as was the case for the hexagonal lattice in [13]. The $n = 7$ illustrations show a seven sided sector like growth and a circular appearance which has not been seen in the hexagonal case. This is particularly interesting given the longstanding search for automata exhibiting circular growth [15]. The $n = 8$ illustrations exhibit dendritic and sector growth with D_8 symmetry. Although this form appears very natural, it is not compatible with ordinary crystalline structures.

Parameter diagrams like those in Figure 3 for the $n = 6,7,$ and 8 cases are not surprising given our experience with the hexagonal lattice and $n = 5$ quasicrystalline structures. When $\gamma = 1$ and for all β, we see regular n-gons when n is even; however, for the same values of γ and β we see $2n$-gons when n is odd. This is due to the double branching that occurs in cases where n is odd. In general, larger β and γ resulted in fuller growth with dendrite growth resulting when β is intermediate and γ is low. In the odd dimensions we see clump like growth for large β and low γ. On occasion that growth appears to be remarkably circular.

Variations on Center

The global symmetry can be destroyed by using a different shift in constructing the structure. Varying the position of the starting point of the growth model also breaks the symmetry. In this case, the same basic growth patterns of stellar, dendritic, and plate forms are observed on the different quasicrystalline lattices. However the patterns are usually dramatically less symmetric. When the value γ is near 1, the forms resemble

regular polygons as can be seen on [14]. In other cases there appears to be a significant random component to the growth which is an expression of the irregular nature of the quasicrystalline structure.

The first illustration of Figure 8 shows a growth structure with a highly random appearance much like DLA dendrtic growth. On careful inspection, the 5 dominant directions of the underlying quasicrystalline structure can be seen in the directions of the branches. The second illustration shows much fuller growth and illustrates that if the initial seed is placed on a vertex with reflective symmetry on the quasicrystalline structure, the growth will maintain the reflective symmetry. Thus some, but not all, of the symmetry of the quasicrystalline structure may be maintained by the growth. The $n = 7$ illustration shows a structure similar to DLA structures and the bias in branch directions is no longer visually apparent. The $n = 8$ case shows a structure in which the growth seems to have dihedral D_1 symmetry, but careful inspection reveals that it is not symmetric. The growth branches are dendrites and their direction exhibits the underlying quasicrystalline structure. Additional examples of growth of these random growth patterns from Z_5 and Z_7 quasicrystals can be found on [14].

Cyclic Growth

We have seen that we could produce growth with a reflection symmetry on a D_n symmetric quasicrystalline structure by selecting initial seeds in specific positions. We are interested in whether we can produce cyclic, but not dihedral, growth with constructions like we have used. In particular, we would be interested in initial placements or restrictions of the structure that produce the desired cyclic growth. We

have not found a simple mechanism for accomplishing that, but can produce the *n*-fold cyclic growth by introducing bias on the weights used in the local averaging. The weights are determined using information about the global position of the patch, and hence this modified technique is not a local automaton in strongest sense. However, each vertex is updated in a consistent manner using only information from a fixed local patch.

In order to obtain cyclic growth we modify our averaging scheme that is used on the nonreceptive material. The averaging scheme is designed as follows: suppose a vertex *v* has neighbors v_i and that those neighbors have polar angle θ_i as measured using the center of symmetry for the origin. Also let θ be the polar angle of *v* and let $\Delta\theta_i = \theta - \theta_i$. The weight associated with the neighbor vertex v_i is proportional to $\Delta\theta_i - \min(\Delta\theta_j) + \varepsilon$ where the minimum ranges over *j* so that each neighbor of the *v* is considered and the parameter ε controls the cyclic bias. The proportion is chosen so that the weights from all the neighbors of *v* sum to one. As before, the contribution of the nonreceptive portion is ½ of the value of the cell plus ½ the average (in this case weighted) value of its neighbors. When $\varepsilon = \infty$, the weights will be equal and hence this corresponds to the ordinary averaging scheme. When $\varepsilon = 0$ the vertex with smallest θ_i will be given zero weight. Hence, these are the extremes where we expect dihedral and highly biased growth. To simplify the initialization, we use equal weight averages for the center and each of the neighbors of the center.

Figure 9 shows the growth that occurs for several ε when $n = 8$, $\beta = 0.35$ and $\gamma = 0.0001$. First, we see the fully dihedral 8-fold symmetric growth. Then $\varepsilon = 64$ shows growth that is slightly asymmetric, but the main features of the dihedral growth are still quite visible. When $\varepsilon = 0.6484$ we see the growth has become quite asymmetric. By

$\varepsilon = 0.1098$ we see the growth has begun to swirl. The further examples show even more extreme swirling. Other illustrations and animations may be found at [14].

Conclusions

Previous investigations have produced models of crystal growth with 6-fold symmetry that exhibit dendritic, sector, stellar and plate forms. Crystalline structures cannot have general *n*-fold rotational symmetry; however, quasicrystals can be produced with global *n*-fold symmetry. This investigation shows that models on suitable quasicrystalline structures can create all those growth forms with any *n*-fold symmetry. Moreover, this model produces new forms: graupel-like forms and growth similar to probabilistic DLA growth.

Ackknowledgement

This work was supported in part by a Lafayette College Excel grant.

References

[1] E. Berlekamp, J. Conway, and R. Guy. Winning ways for your mathematical plays. Academic Press, New York, 1982.

[2] Callahan P. Paul's page of Conway's life miscellany. http://www.radicaleye.com/lifepage/lifepage.html.

[3] Wolfram S. A new kind of science. Champaign: Wolfram Media; 2002.

[4] Russ JC. The image processing handbook, fourth ed. Boca Raton: CRC Press; 2002

[5] Reiter CA. A local cellular model for snow crystal growth, Chaos, Solutions and Fractals, to appear.

[6] Senechal M. Quasicrystals and geometry. Cambridge University Press; 1995.

[7] Barabasi A–L, Stanley HE. Fractal concepts in surface growth. Cambridge University Press; 1995.

[8] Vicsek T. Fractal growth phenomena, second ed. World Scientific.Singapore 1992.

[9] Weeks E. Cellular automata on quasicrystals, http://www.physics.emory.edu/~weeks/pics/qvote3.html.

[10] Bentley WA, Humphreys WJ. Snow crystals. McGraw-Hill Book Company; 1931. Also, New York: Dover Publications; 1962.

[11] Libbrecht K, Rasmussen P. The snowflake: winter's secret beauty. Stillwater: Voyageur Press; 2003. Auxiliary: http://www.snowcrystals.com.

[12] Nakaya U. Snow crystals: natural and artificial. Harvard University Press; 1954.

[13] Reiter CA. Atlas of quasicrystalline tilings, Chaos, Solutions and Fractals 14 (2002) 937-963.

[14] Chidyagwai P, Reiter CA. Auxiliary materials for: a local cellular model for growth on quasicrystals, http://ww2.lafayette.edu/~reiterc/mvp/qcgm/index.html.

[15] Gray L. A mathematician looks at Wolfram's new kind of science, Notices of the AMS 50 (2003) 200-211.

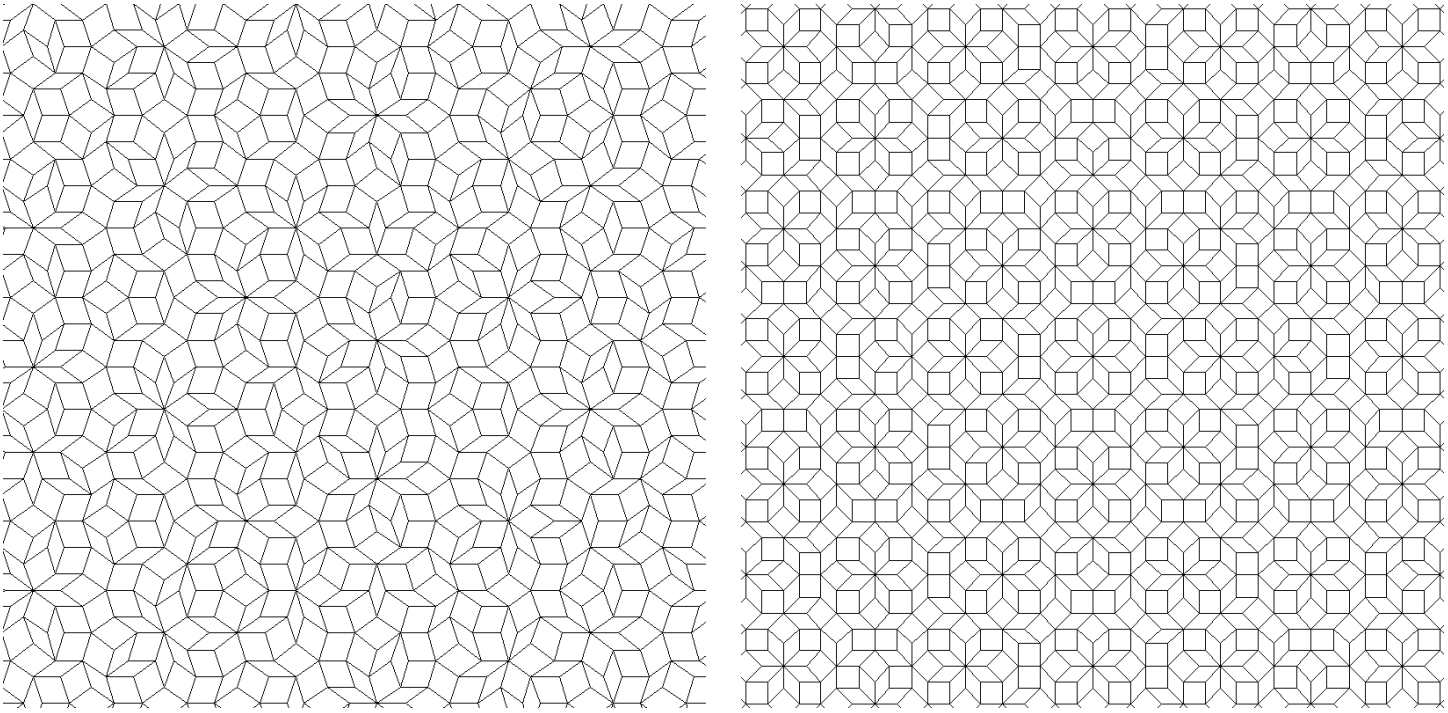

Figure 1. Quasicrystalline structures from Z_5 and Z_8

.

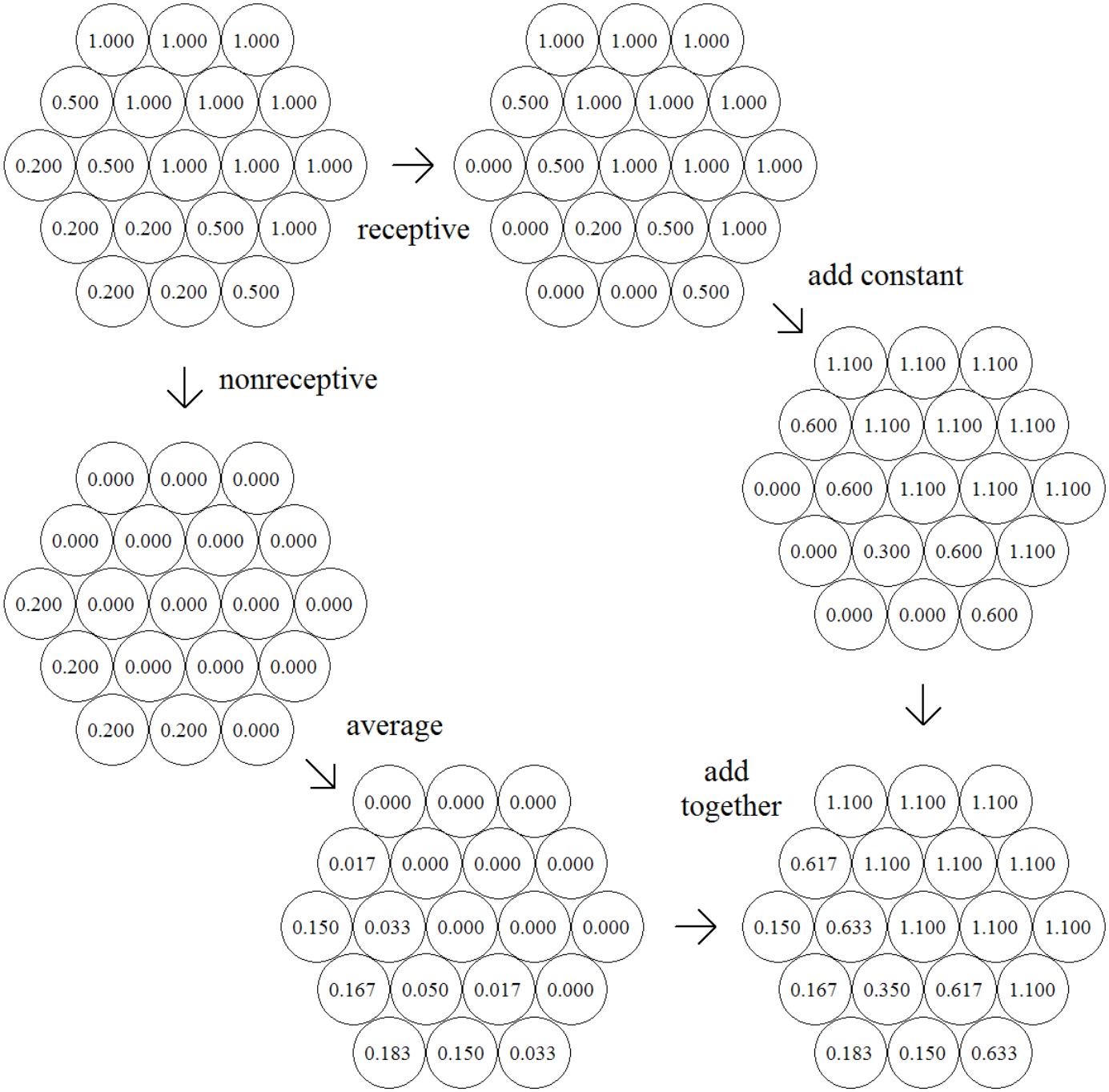

Figure2. Illustration of the growth model on a small hexagonal patch.

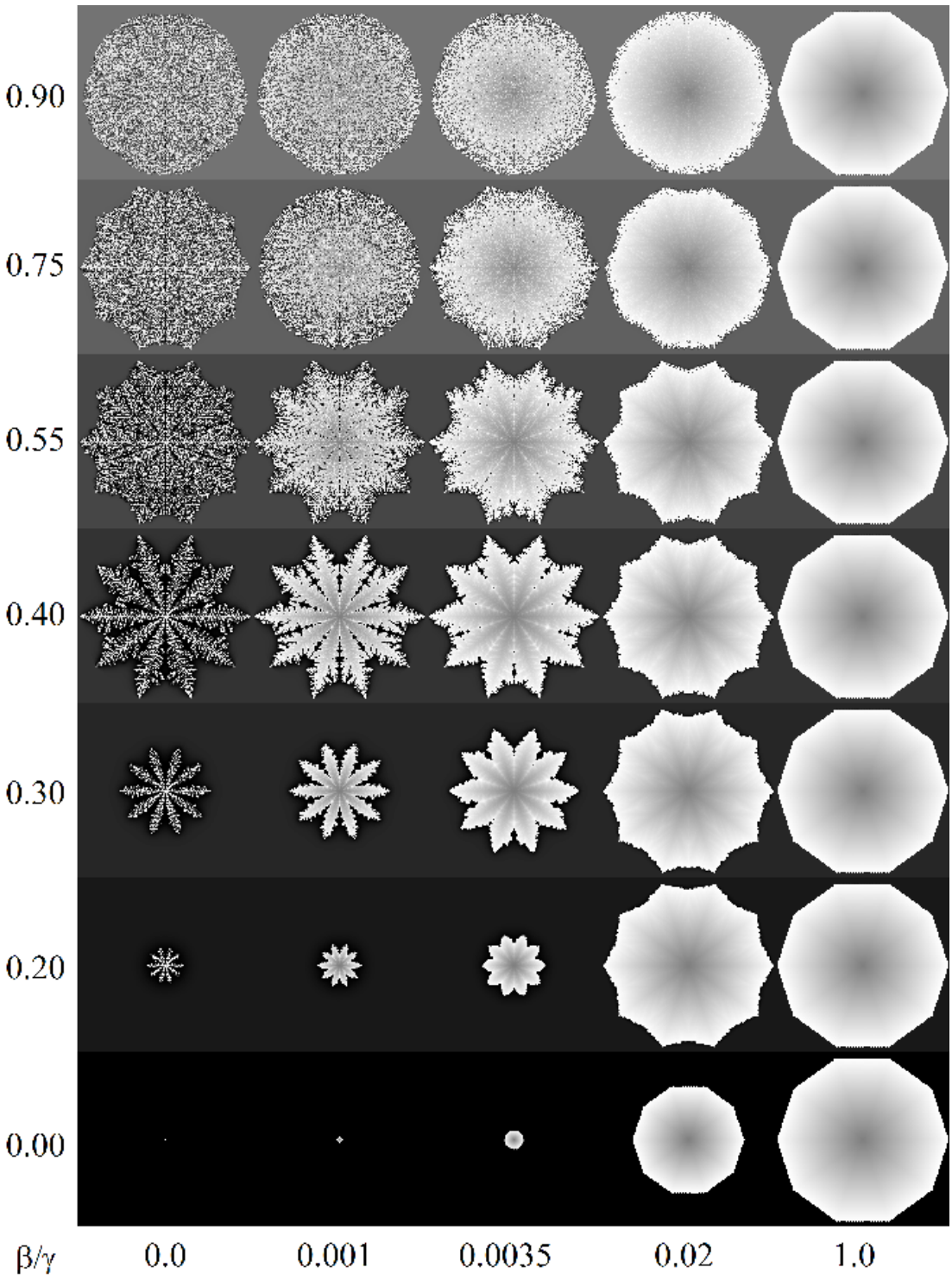

Figure 3. Growth forms on quasicrystals from Z_5 that appear as β and γ vary.

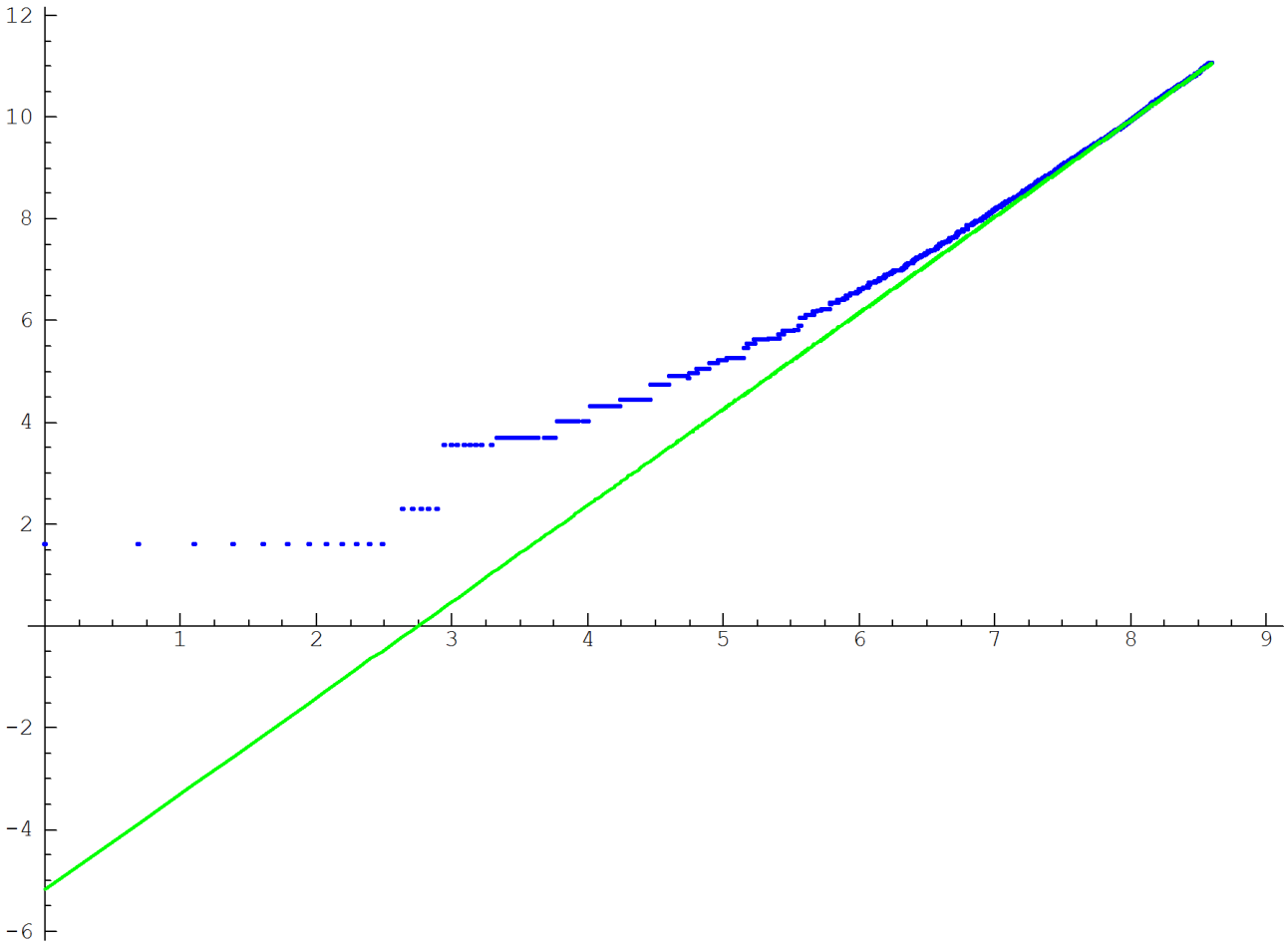

Figure 4. A log-log plot of number of edge positions versus time for dendrite growth.

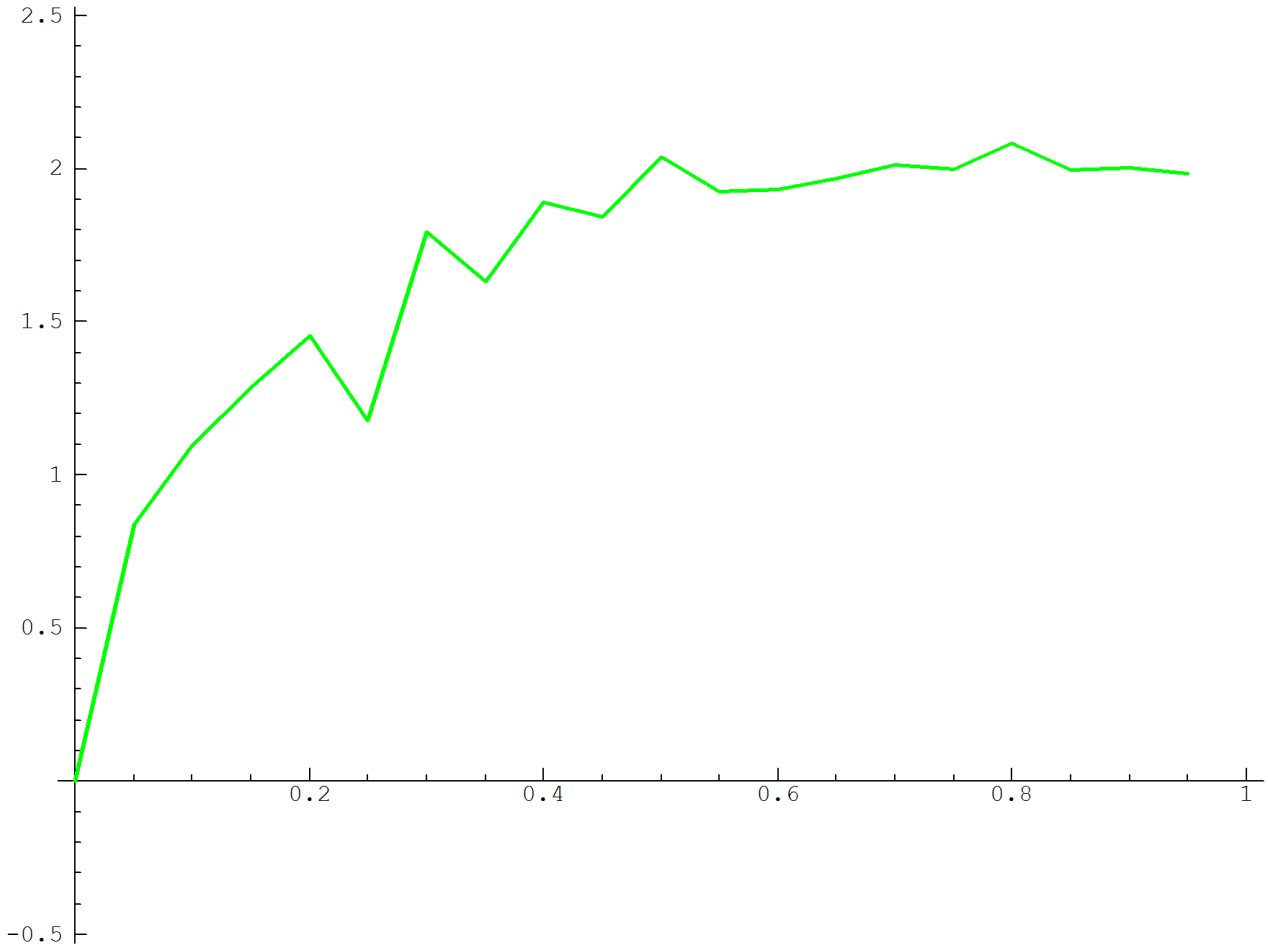

Figure 5. Fractional exponent of the number of edge cells versus β for $\gamma = 0$

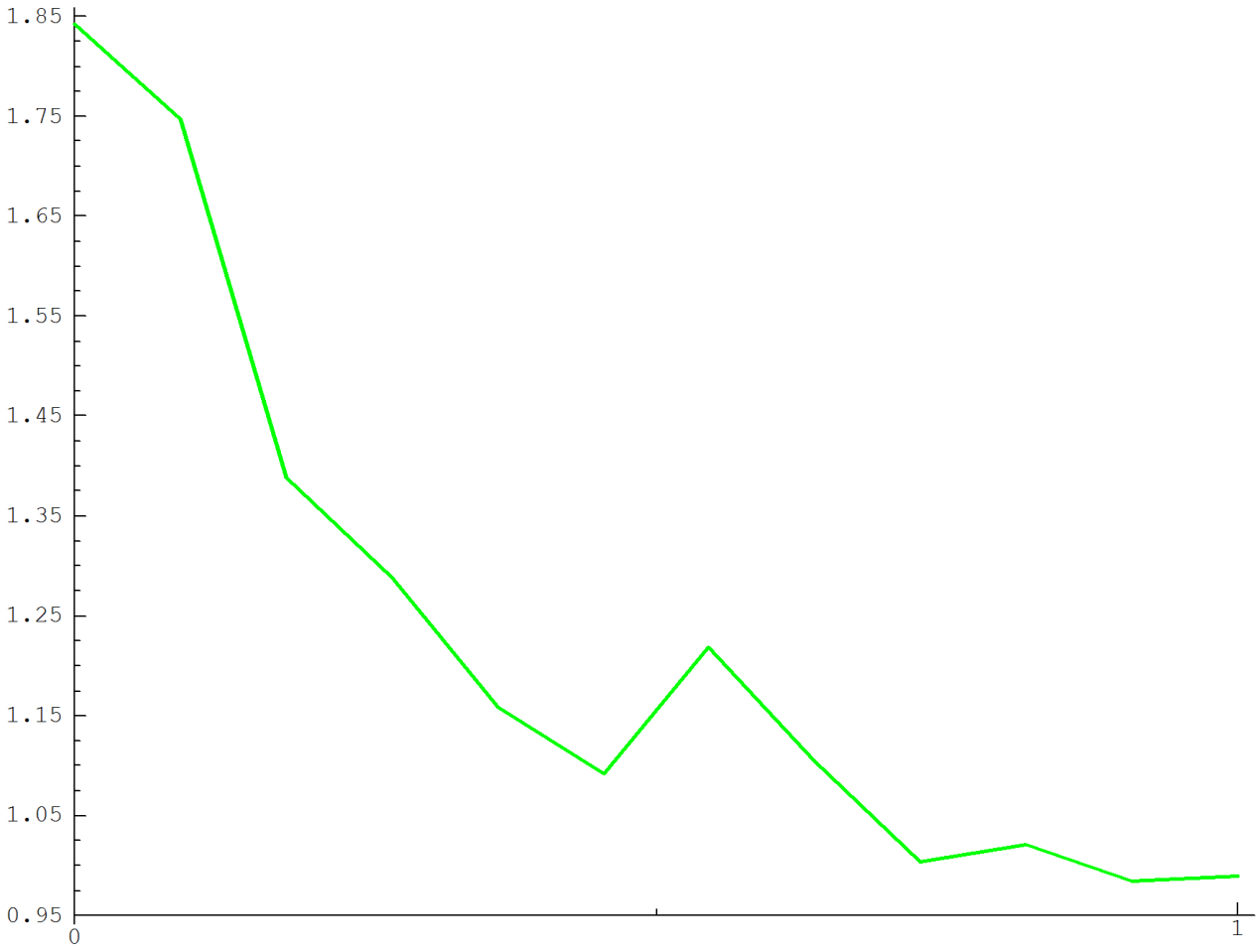

Figure 6. Fractional exponent of the number of edge cells versus γ for $\beta = 0.45$

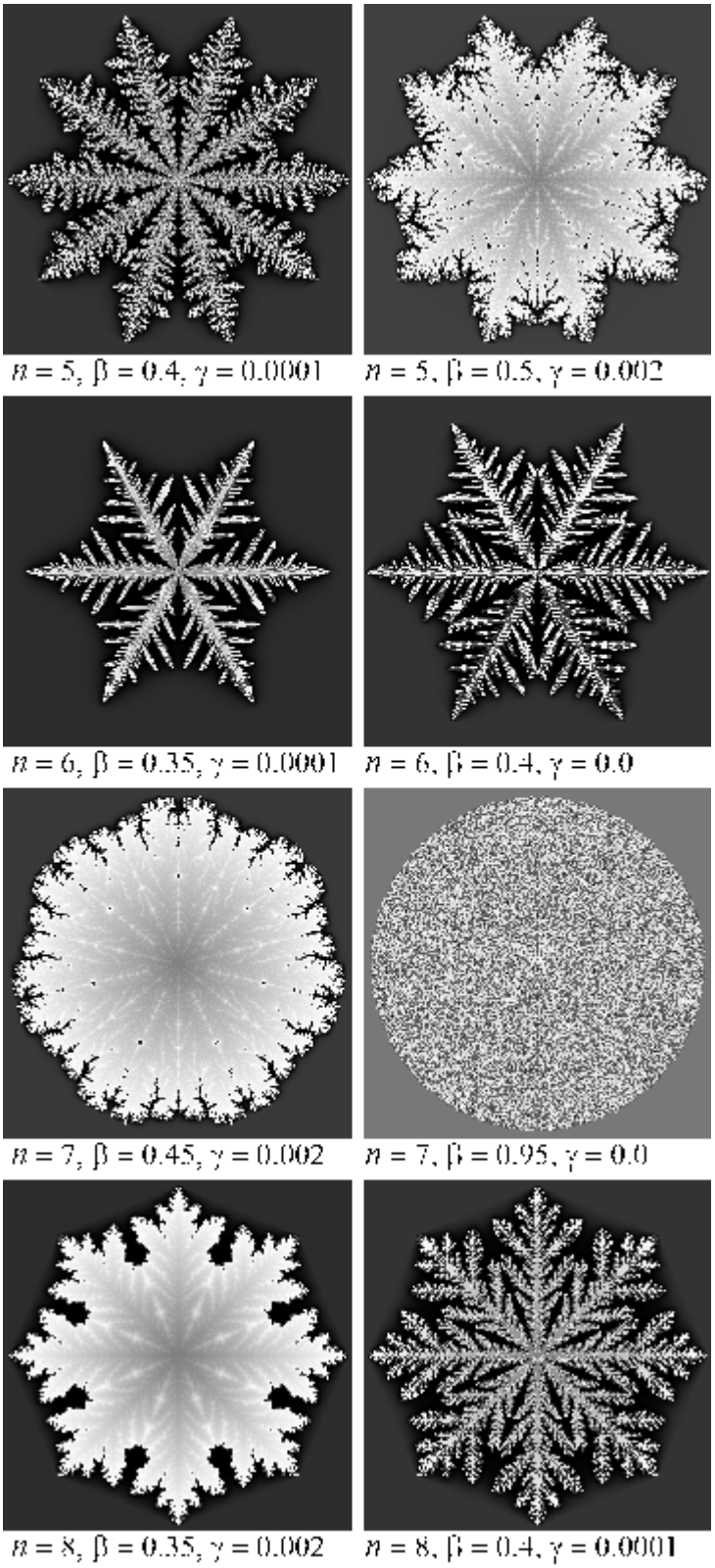

Figure 7. Growth forms on quasicrystals from Z_5, Z_6, Z_7, and Z_8.

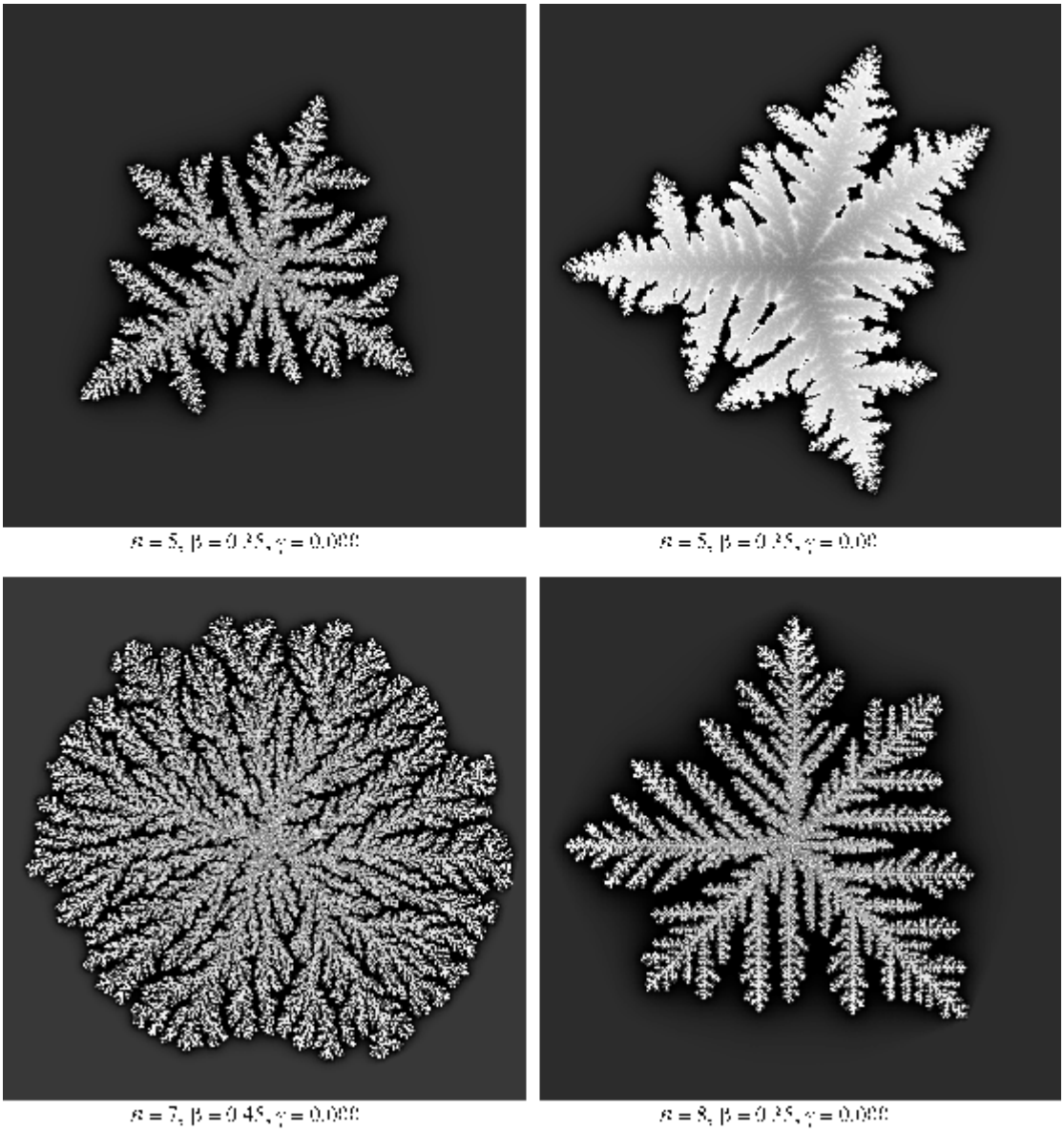

Figure 8. Growth with a noncentral seed

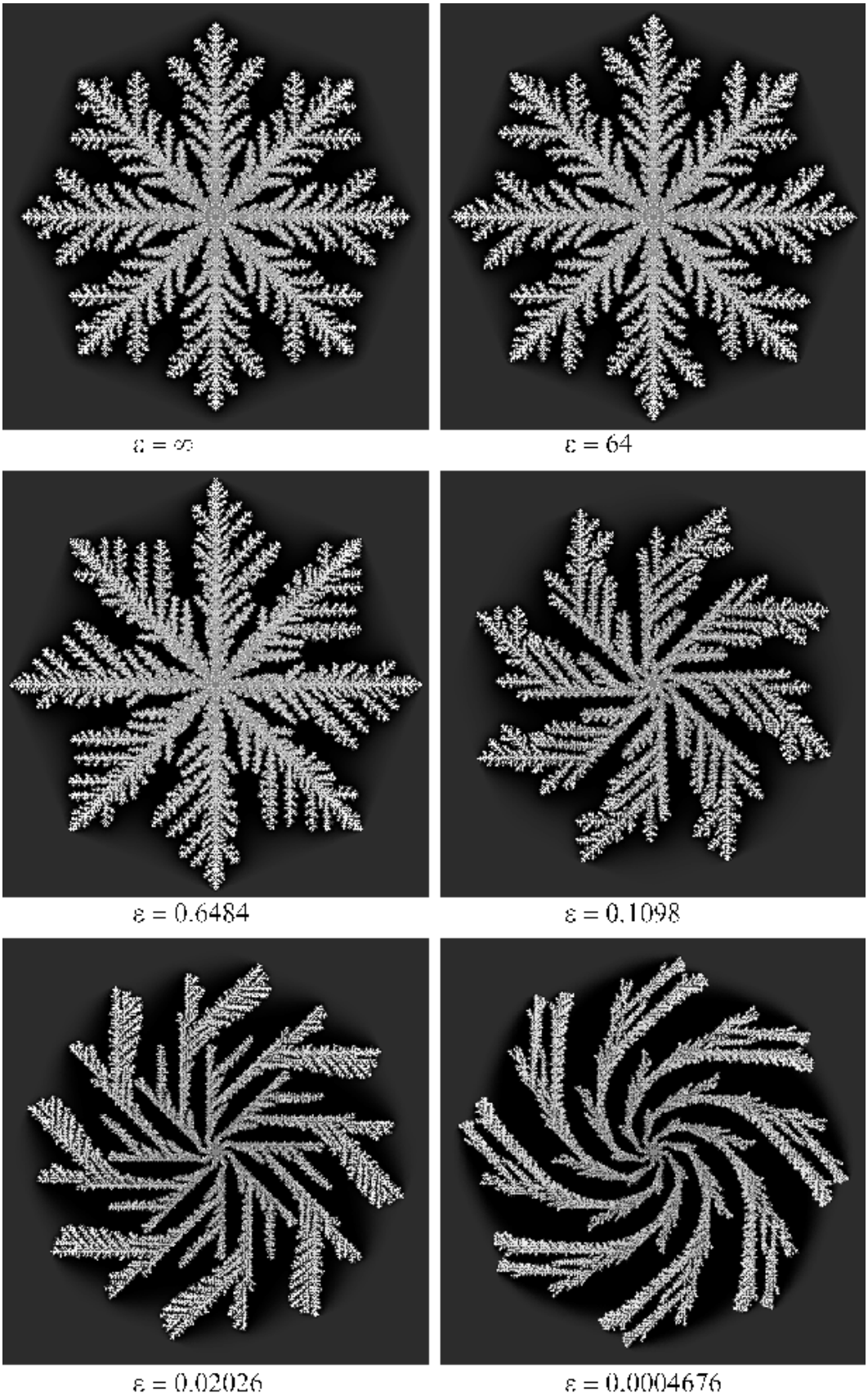

Figure 9. Cyclic growth with several bias values.